5.4 CHARACTERISICS OF SPRITE-PRODUCING ELECTRICAL STORMS IN THE STEPS 2000 DOMAIN

Walter A. Lyons, CCM*, Laura Andersen, Thomas E. Nelson
Yucca Ridge Field Station, FMA Research, Inc, Fort Collins, Colorado

Gary R. Huffines
University of Northern Colorado, Greeley, Colorado

1. INTRODUCTION

The unanticipated discovery of red sprites in 1989 changed forever our view of the interactions between tropospheric electrical activity and middle atmospheric optical phenomena (Franz et al. 1990; Lyons and Armstrong 2004). Once thought to be electrically quiescent, the stratosphere and mesosphere are increasingly found to be the home to a growing variety of lightning-related electrical discharges and intense transient electric fields (Lyons 2006). The discovery of literal cloud-to-stratosphere electrical discharges from intense thunderstorm tops, including blue jets, giant jets and true upward lightning (Lyons et al. 2004a) continues to engender the need for intensive investigations of this region. However, the relative scarcity and apparently random nature of cloud top discharge events make them difficulty to study in a systematic manner. Red sprites, and to a lesser extent elves (Fukunishi et al. 1996) and halos (Barrington-Leigh 1999), by contrast, are increasingly well understood and predictable. During the summer of 2000, a major field program, the Severe Thunderstorm Electrification and Precipitation Study (STEPS) was conducted on the U.S. High Plains. While its focus was on supercell convection, the experimental design also allowed for detailed investigations of mesoscale convective systems (MCSs). Over continental regions, sprites are known to frequently occur in association with positive cloud-to-ground (+CG) strokes in MCSs (Lyons 1996; Lyons et al. 2000), although even in the most productive storms rarely do more than 1 in 5 +CGs trigger a sprite. Theoretical research into red sprite production has seen the proposal and disposal of a number of theories (Wilson, 1925; Rodger 1999). At the current time, sprites are generally agreed to be the result of conventional dielectric breakdown at approximately 70-75 km height, the result of a strong transient electrical field resulting from the removal to ground of large amounts of electrical charge in a CG flash (Pasko et al. 1996, 1998). Though this theory is not polarity dependant, the vast majority of sprite parent CGs are positive (SP+CGs), with only two documented –CG events on record (Barrington-Leigh et al. 1999). While the peak current of SP+CGs is typically 50% larger than the other +CGs in the same storm (Lyons et al. 2003b; Lyons 1996), the peak current by itself is not a good predictor of sprite formation. As initially suggested by C.T.R. Wilson (1925), the key metric is the charge moment change:

$$\Delta M_q(t) = Z_q \times Q(t) \qquad (1)$$

defined as the product of Z_q, the mean altitude (AGL) from which the charge is lowered to ground, and the amount of charge lowered. Note that this second term is most appropriately considered as a function of time. New measurement techniques (Cummer and Lyons, 2004 and 2005) can now routinely monitor the impulsive charge moment change ($i\Delta M_q$), which is that produced by the charge lowered in roughly the first 2 ms of the CG. This is often dominated by the return stroke plus the initial stages of any continuing current.

Huang et al. (1999) and Williams (2001) refined Wilson's original theory and proposed, based upon initial measurements gleaned from Schumann resonance ELF transient analyses (Boccippio et al. 1995), that for such breakdown to occur, total ΔM_q values would need to be on the order of 300 to 1000 C km. These values are many times larger than what have been believed to be the "normal" values for ΔM_q (Rakov and Uman 2003). The STEPS program provided ideal circumstances to delve into the characteristics of MCS SP+CGs strokes. The key question to be addressed: What is different about those +CGs which trigger sprites? Where in the storms, and during what phase of its life cycle, do these unusual discharges occur?

ELF-based remote sensing methods for the characterization of lightning charge moment changes based upon the concepts proposed by Cummer and Inan (1999), and as exploited for STEPS data by Cummer and Lyons (2004, 2005) has detailed that ΔM_q and even $i\Delta M_q$ (if properly employed) can provide a very useful threshold to discriminate between those +CGs which produce sprites (and elves and halos) and those which do not. In this paper we will investigate the characteristics of those TLE-producing storms as observed using conventional NLDN data (Cummins et al. 1998), GOES satellite and NEXRAD radar reflectivity. We will first review the

* *Corresponding Author Address*: Walter A. Lyons, CCM, FMA Research, Inc. 46050 Weld County Rd 13, Ft. Collins, CO 80524; e-mail: walyons@frii.com, www.FMA-Research.com; www.Sky-Fire.TV

STEPS program and discuss a prototypical sprite-producing MCS and a typical sprite-producing +CG.

2. STEPS 2000

The STEPS program was conducted on the High Plains of eastern Colorado, western Kansas and southwest Nebraska from 22 May through 16 July 2000. The observation program was designed for coordinated measurements of the dynamical, microphysical and electrical processes within several classes of severe storms, especially those producing positive CGs. Lang et al. (2004) provide a complete description of the field program resources and some initial results.

Most relevant to our efforts was that STEPS deployed an operational 3-D Lightning Mapping Array (LMA), which provided information on intracloud discharges to ranges approaching 100-150 km (for 3-D mapping) and 150-300 km (for 2-D mapping) (Thomas et al. 2004). Centered near Goodland, KS, the LMA domain was ideally situated to allow for monitoring sprites and other transient luminous events using a suite of low-light television cameras (LLTVs) and photometers. These were deployed some 275 km to the northwest at the Yucca Ridge Field Station (YRFS) outside of Ft. Collins, CO. During the campaign, over 1200 TLEs were documented, with over 50 within the prime coverage area of the LMA. Coincident with the optical monitoring, ELF transients were recorded by both MIT (Earle Williams) and Duke University (Steven Cummer) for the purpose of extracting ΔM_q values for the CGs occurring within the storms of interest. This represented the first large scale effort to determine not only lightning polarity and peak current within these storms, but also ΔM_q, and for events within the LMA, Z_q and the computed charge (Q) lowered to ground. It also facilitated further testing the hypothesis of Lyons (1996) that SP+CGs tended to be largely confined to portions of the stratiform precipitation region of MCSs, generally in areas with reflectivities <20-40 dBZ, once this region had attained a size of >1-2x10^4 km^2. In addition, Williams (1998) had proposed that the SP+CGs were most likely associated with charge removal (Z_q) from the lower stratiform charge layers, in the 0° to -10°C region. This contrasts sharply with the numerous theoretical modeling papers of sprite energetics which postulated Z_q values between 10 and 20 km, in part to allow for generation of sufficiently large ΔM_q to trigger mesospheric breakdown (Rowland 1998).

During STEPS, the Duke ELF system obtained the ΔM_q values for a large number SP+CGs. For those events with moderately long CG-to-sprite onset time delays of ~6-10 ms, little correlation between peak current and ΔM_q could be found (Lyons et al 2004). This is consistent with the notion that for sprites with time delays greater than several milliseconds after the SP+CG much of the charge transfer occurs after the initial return stroke (as measured by the NLDN), and is accomplished by continuing currents of considerable magnitude (likely fed by the extensive dendrite patterns of spider lightning spreading outward into the large laminae of positive charge found in the MCS stratiform region). Most interesting, a probability distribution of ΔM_q threshold values suggested there was a 10% chance of a sprite for +CGs of 600 C km, increasing to 90% for values of 1000 C km or larger (Hu et al. 2001).

3. 19 JULY 2000: A PROTYPICAL SPRITE-PRODUCING MCS.

Two modest size mesoscale convective systems (MCS) passed through the LMA domain on 19 July 2000. Two techniques of estimating changes in vertical charge moment (ΔM_q) yielded averages of ~800 C km (Duke) and ~950 C km (MIT) for 13 sprite-parent +CGs (Lyons et al. 200b). Analyses of the LMA's VHF lightning emissions within the two mesoscale convective systems (MCS) show +CGs did not produce sprites until the mature phase of the storm when the stratiform region grew to >3x10^4 km^2. Moreover, the centroid of the maximum density of VHF lightning radiation emissions dropped from the upper part of the storm (7-11.5 km AGL) to much lower altitudes (2 - 5 km AGL) (Fig. 1). The average height of charge removal (Z_q) from the sprite-parent +CGs during the late mature phase of one MCS was 4.1 km AGL. Thus, the total charges lowered by sprite parent +CGs were on the order of 200 C (maximum 345 C). The average area from which charge was removed was ~1300 km^2. These cases are supportive of the conceptual MCS sprite production models previously proposed by Lyons (1996) and Williams (1998).

Figures 2 – 5 portray this MCS at the time of one of the SP+CGs presented here in more detail. The +CG event, a 30 kA stroke, occurred at 0600.15.364 UTC. The sprite was rather dim and occurred more than 100 ms after the CG return stroke, indicating a significant role for the continuing current. This is an example of a "long delay" sprite. There are numerous events which appear to occur well under 10 ms after the CG and can be considered "short delay", indicating a more impulsive nature of the parent CG and a greater role for the return stroke and the contribution of the immediately following continuing current to the charge moment change. This CG was associated with a total ΔM_q of 525 C km (as detected by the MIT ELF system). The SP+CG is shown (red lighting bolt) in the GOES Infrared image. We note the sprite occurred above the cold, but not the coldest, part of the MCS cloud canopy (-75°C as indicated by the white area). The SP+CG occurred in the low reflectivity (25 dBZ) portion of the stratiform precipitation, in this case located mostly north of the southeast moving convective core, which had a peak reflectivity of >60 dBZ. Figure 4 shows the CG pattern from the NLDN, in which the convective core was dominated by almost exclusively negative CGs (green dots), with the +CGs (blue crosses) populating the stratiform region. The +CGs producing sprites are indicated with red crosses, with the western-most event being the 0600.15.364 UTC event.

Figure 5 shows a ten minute (0550-0600 UTC) compilation of the VHF source density as monitored by the LMA. The VHF source density in the convective core is two orders of magnitude greater than those occurring in the region of sprite generation. SP+CGs are often found in the low reflectivity portions of the storm, having modest rates of VHS electrical activity. Those SP+CGs which do occur exhibit extremely large ΔM_q values.

Figure 6 is a newly designed LMA display used for ongoing investigations of lightning discharges generating sprites. The time line is centered on the +CG event time, and extends 300 ms before and after, encompassing the duration of the IC discharge. The VHF sources detected before the +CG are plotted in green. Those occurring between the time of the CG and the optically determined onset of the sprite (to within 17 ms video resolution) are shown in yellow. Those VHF sources occurring while the TLE was optically detectable by the LLTV systems are in pink. The grey points are those sources from the tail end of the cloud discharge after the sprite fades.

In the first 100 ms after the CG return stroke, charge appears to be removed from about the 5 km AGL level. During the period of sprite luminosity, the values drop to about 4 km AGL, which is approximately the altitude of the melting layer. We note that the area from which charge appears to have been drawn from the onset of the CG to the end of the sprite luminosity is ~3000 km^2. This is larger than the original estimate presented in Lyons et al. (2003b). This results from using undecimated (full resolution) LMA data which shows the IC discharge in much greater detail and area coverage.

We also note in the YZ display panel, that there is as clear slope downward of the VHF sources from 8 -10 km at the onset of the IC to about 4-6 km at its termination. This temporal lowering of the altitude of VHF sources is also evident in the ZT panel on the top. Approximately a third of the SP+CGs in this MCS evidenced a discharge which began near the top of the convective core at the south end of the storm and systematically descended to lower altitudes as it moved northwards into the stratiform region. Similar discharge behaviors were found in the MCS of 16 June 2002 as it approached the Dallas-Fort Worth LDAR II 3-D lightning mapping system by Carey et al. (2005.) This finding will be discussed further below.

Note also that the sprite luminosity occurred as the dendritic "spider lightning" branches were systematically propagating tens of kilometers outwards from the +CG attach point. A similar behavior was noted for SP+CGs in MCS storms in Florida by Stanley (1999).

4. CLIMATOGICAL CHARACTERISTICS OF TLE-PARENT CGs

A major effort has been expended in creating a database of High Plains TLE events (primarily sprites), and the characteristics of the NLDN-detected parent CGs and their parent storms (mostly MCSs) as determined by GOES and NEXRAD data. This database includes most events observed during STEPS as well as from selected storms spanning the summers of 1995 through 2004. One squall line and two supercell storms are included, though the majority of events are MCSs with trailing stratiform precipitation regions. Figure 7 plots the parent +CG locations for 2219 TLEs, mostly sprites. The maximum effective detection range of the LLTVs under ideal conditions is about 1000 km. These events are associated with the nocturnal MCSs which routinely traverse the US High Plains during summer. The dearth of TLE detections in Colorado is due to the fact that most summertime orogenic storms have already moved through Colorado as they evolve upscale into MCS convection by the time darkness (0230-0330 UTC in summer) allows LLTV monitoring.

Figure 8 is the distribution of the UTC times during which TLEs have been observed from YRFS, spanning the period from 02-03 UTC (sunset) to 10-11 UTC (sunrise) during summer. The peak observing times are from 0400 to 0700 UTC (10 PM to 1 AM local time). The decrease after 0700 UTC is due to weakening of some storm systems after this time, plus increasing distances and/or cloud obscuration and/or (sometimes) terminated monitoring due to the late hour. It is likely that over the US High Plains, the most active time for sprites, halos and elves is plus or minus two hours of local midnight. (There continue to be no blue jet or giant jet observations in the YRFS database after 12 seasons of observations.)

Most storms, if they produce one TLE, will generally continue for more than two hours, with some continuing for six hours or more (Figure 9). Single TLE events do occur, but are quite uncommon. The typical TLE storm produces on average 70 events (Figure 10). There are, however, some storms which produce substantially larger numbers of TLEs. One generated approximately 750 events in about 3 hours (not part of this subset of our records). The causes of such hyper-active storms are unknown, though Lyons et al. (1998) speculated these storms may be ingesting large amounts of smoke from wildfires.

Most MCSs require several hours before TLE production begins. Using GOES satellite time lapse sequences, we computed the ages of the each system (from when it first became recognizable as an entity) when TLEs were first observed. While a few produced TLEs during their first two or three hours, the majority of the storms were 3 to 8 hours old before activity commenced (Figure 11). This illustrates a long standing forecasting rule of thumb that TLEs most typically are associated with MCSs in their late mature stages.

We next compiled the NLDN stroke data for parent +CGs which produced only optically confirmed sprites (Figure 12a) and those which included elves and halos, some of which were also followed by sprites (Figure12b). Forecasting experience has noted that TLE-producing storms tend to have greater percentages of +CGs than others, but there is great variability from storm to storm (less than 10% to over 90%). One rather consistent feature, however, is that the TLE parent CGs do have higher average peak currents than the other CGs in the same system. For sprite-only events, the average is ~60 kA. However, note the large standard deviation (~35 kA) and the wide range of values (< 10 kA to > 250 kA) illustrating that peak current alone is a poor indicator of TLE potential. For those TLE parent CGs in which elves and halos were involved, the average peak current is even larger, ~115 kA, and again with a large standard deviation of ~46 kA. Thus, the impulsive contribution of the return stroke to the overall charge moment change which, while often substantial, is usually, except in rare cases, insufficient to reach breakdown ΔM_q values for sprites, but may be sufficient sometimes to induce impulsive elves and halos. Evidence is accumulating that some continuing current is almost always involved in TLE production, though the additional contribution may be fairly small when the initial CG return stroke is highly impulsive.

The likely role of continuing currents is illustrated by analysis of the delay times between the NLDN-determined CG return stroke and the onset of TLE luminosity using LLTVs. While the +CG time is known to 1 ms precision, the temporal resolution of video fields is 16.7 ms, greatly reducing the precision to which the delay time can be calculated. However, in many cases the CG occurs after the onset of the video integration period, and thus delay times shorter than 16.7 ms can be inferred for some events. For this paper, the delay time is the sum of the earliest time the sprite could have begun in the video plus 16.7 ms (the field integration time) divided by 2. For sprite-only TLEs, the distribution of estimated delay times is shown in Figure 13. The distribution is very broad with a mean of ~32 ms and a standard deviation of ~46 ms. There are a considerable number of events that occurred in less than 16.7 ms after the CG. Many of these are the “short delay” sprites in which the impulsive charge moment change from the CG required only a little additional continuing current in order to achieve dielectric breakdown at mesospheric altitudes. Some events, however, can be many tens of or even >100 ms, indicating the need for considerable continuing current in order to achieve the required ΔM_q for mesospheric breakdown “long delay” sprites. Figure 14, a plot of the estimated TLE (sprites, elves, halos) delay times versus NLDN peak current, illustrates that a large CG peak current is helpful in initiating “short delay” TLEs. However, the fact that the large majority of large peak current CGs, especially negative events over land, do not produce TLEs suggests the CG return stroke alone is rarely sufficient to initiate breakdown.

5. CLIMATOGICAL CHARACTERISTICS OF TLE-PRODUCING STORMS

TLEs have been observed above a wide variety of convective systems including MCSs, squall lines, tropical cyclones, winter snow squalls and (rarely) supercells (Lyons 2006). But the vast majority of convective storms do not produce TLEs. Over the central U.S., the most prolific TLE generators are mature MCSs, especially those with significant trailing stratiform precipitation regions. We next examine the characteristics of TLE parent CGs with respect to the convective cloud canopy as determined by GOES infrared satellite data. TLEs generally occur within 50 km of their parent CG (Lyons 1996). The NLDN-derived latitude and longitude provides a reasonable surrogate for the TLE location. Figure 15 shows the distribution of IR cloud top canopy temperatures for High Plains summertime events. It is apparent that TLEs are largely confined to regions of cold cloud tops, with an average of ~-65°C. These values approximate the typical tropopause temperature for the study region during summer. However, the TLEs usually do not occur beneath the *coldest* part of the storm, which is often marked by convective overshooting domes associated with strong convective core updrafts. Figure 16 displays the distribution of coldest cloud tops anywhere within a TLE-producing system. IR cloud top temperatures of -70°C and even -75°C are present in the majority of convective systems producing sprites. The warmest value noted in almost 100 periods of 30 minutes each was -55°C.

Long term forecasting experience has also noted that over the central U.S., TLEs rarely are associated with smaller convective systems. The distribution of the number of TLEs versus the total area of the storm cloud shield (an IR temperature typically around -30°C) is shown in Figure 17. No system smaller than 20,000 km^2 has been observed which was producing sprites. It appears that a cloud top temperature of -50°C or -55°C or colder is a necessary, though not sufficient requirement for a convective system over the U.S. High Plains during summer to generate CGs, which in turn trigger TLEs. Only 4 storms with a -50°C cloud top canopy area of <20,000 km^2 were found to produce TLEs (Figure 18). We would note that to adjust these results for application in different seasons and locales, the cloud top temperatures would need to be compared to prevailing tropopause temperatures.

Using regional NEXRAD mosaics available at 30 minute intervals, we compared NLND-reported locations of the TLE parent CG to the reflectivity. We note that the lack of temporal coincidence introduces error in the reflectivity determination, but the rather large and fairly homogeneous nature of the patterns in MCSs tends to minimize this shortcoming. Figure 19 shows that TLE parent CGs occur with reflectivity values ranging from 5 dBZ to 65 dBZ. There is, however, a strong preference for the parent CGs to be located outside of the convective cores (> 55 dBZ), and being most frequent in the 25 - 45 dBZ range, with the mode value being 35 dBZ. These are values typically associated with secondary precipitation maxima and bright band zones in trailing stratiform regions. Indeed, experience has shown that while TLEs do sometimes occur within convective cores, they are most often concentrated in a portion of the trailing stratiform, often quite close to the trailing edge.

We also examined the maximum reflectivity anywhere in the convective system while it was producing TLEs. As shown in Figure 20, it appears a necessary, though not sufficient condition for High Plains storms to generate sprites is a core reflectivity of at least 55 dBZ with values of 65 dBZ and 70 dBZ being common.

The size of the contiguous precipitation region is also a rather robust requirement. Only a small number of TLEs have been monitored above storms in which the 10 dBZ area was <15,000 km^2 (and these were mostly from decaying supercells). For MCSs to have a potential for TLE production, the echo area usually requires a minimum of ~20,000 km^2. It should also contain a fairly large region of stratiform precipitation with values >25-30 dBZ. Convective cores (>50-55 dBZ) are always present, and can range to as large as 15,000 km^2 (Figure 22).

The special qualities of the +CGs which occur in the MCS trailing stratiform can be inferred from Figure 23. Each TLE was assigned a subjectively-determined relative brightness level on the LLTV video from 1 (dimmest) to 5 (upper 20% of luminosity). When the relative brightness is compared to the parent +CGs associated reflectivity, it is clear that the brightest and, it is suspected, the shortest delay sprites occur in the more modest reflectivity regions of the storm (30 dBZ). Very few extremely bright events were noted in or near the convective cores.

5. DISCUSION AND CONCLUSIONS.

By investigating over 2000 TLEs (mostly sprites) from over 3 dozen storms (mostly MCSs with trailing stratiform precipitation regions), a clear picture emerges. The +CGs having sufficiently large ΔM_q values to induce dielectric breakdown in the mesosphere are most likely to occur in a portion of the trailing stratiform where reflectivities are usually <20 - 45 dBZ, with the brightest occurring most frequently above the 30 dBZ area. TLEs in the convective core are not commonly observed. The MCS radar echo must achieve a minimum 10 dBZ area coverage of about 20,000 km^2. The TLE parent CGs occur beneath the colder parts of the cloud canopy, but rarely beneath the coldest portion of the storm top.

Another robust finding for High Plains summer MCS systems was that in order for TLEs to occur, the highest reflectivity in the storm core needed to exceed 55 dBZ. Also the coldest cloud top temperature (for the summer continental U.S. tropopause) was colder than -55°C, and often as cold as -70°C to -75°C.

At first glance the findings that the preponderance of TLEs occur at lower level (perhaps near the melting layer) in the weaker reflectivity portions of the trailing stratiform are contradictory with the need for tall, intense convective cores. Yet our understanding of the dynamics and electrical nature of leading-line, trailing-stratiform MCSs are rapidly improving (Demetriades et al. 2004; Davis et al. 2004; Carey et al. 2005). Figure 23, from the recent paper by Carey et al. (2005), presents a conceptual illustration of the complex, elevated front-to-rear and low-level rear-to-front flows behind advancing MCS convective lines. Most intriguing was the finding that a number of lightning discharges in one case study initiated near the top of the convective core and then sloped rearward and downward into the bright band region. While it was not known if any of these flashes produced TLEs, this is the behavior of a sprite parent flash illustrated in Figure 6 of this paper. The schematic suggests positively charged ice mass may be distributed upward and then rearward, settling through the regional mesoscale updraft and into the bright band with one or more associated large horizontal laminae of positive charge. Charge advection within such storms may indeed play a role comparable with that of *in situ* charge generation (Schuur and Rutledge 2000). Only relatively brief intervals (typically on the order of an hour) are needed in which TLEs often cease when MCS convective cores fall below “severe” limits (55 dBZ) and cloud tops warm below ~-55°C. This may indicate that the extensive front-to-rear descending IC discharges from atop the deep convective core subsequently trigger the large +CG followed by the spider lightning which taps the positive charge reservoir near the bright band to create large ΔM_q values in the prototypical MCS sprite event.

6. ACKNOWLEDGEMENTS

This work has been supported by the National Science Foundation, Physical Meteorology and Aeronomy Programs (ATM - 0000569, ATM - 0221512). We very much appreciate the considerable assistance provided by Russ Armstrong, Steven Cummer, Liv Nordem Lyons, Mark Stanley, David Suszcynsky, Victor Pasko, Earle Williams, and our summer interns from the University of Northern Colorado: Judy Fossum, Alicia Faires and Katie Burtis The LMA data and assistance in its interpretation were graciously provided by New Mexico Tech (Paul Krehbiel, Bill Rison, Timothy Hamlin and Jeremiah Harlin). We gratefully acknowledge the contribution of NLDN lightning data to STEPS investigators by Kenneth Cummins, Vaisala, Inc.

7. REFERENCES

Barrington-Leigh, C.P., U.S. Inan, M. Stanley and S.A. Cummer, 1999: Sprites directly triggered by negative lightning discharges. *Geophys. Res. Lett.,* **26**, 3605-3608.

Boccippio, D.J., E.R. Williams, W.A. Lyons, I. Baker and R. Boldi, 1995: Sprites, ELF transients and positive ground strokes. *Science*, **269**, 1088-1091.

Carey, L.D., M.J. Murphy, T.L. McCormick and N.W.S. Demetriades, 2005: Lightning location relative to storm structure in a leading-line, trailing-stratiform mesoscale convective system. *J. Geophys. Res*., **110**, D03105m doi: 10.1029/2003JD004371.

Cummer S.A., N. Jaugey, J. Li, W.A. Lyons, T.E. Nelson and E.A. Gerken, 2006: Submillisecond imaging of sprite development and structure. *Geophys. Res. Lett* (submitted).

Cummer, S.A. and W.A. Lyons, 2005: Implications of lightning charge moment changes for sprite initiation. *J. Geophys. Res*., **110**, A04304, doi:10.1029/2004JA010812.

Cummer, S.A. and W. A. Lyons, 2004a: Lightning charge moment changes in U.S. High Plains thunderstorms. *Geophys. Res. Lett.,***31**, L05114, doe:10.1029/2003GL019043,2004.

Cummer, S.A. and U.S. Inan, 2000: Modeling ELF radio atmospheric propagation and extracting lightning currents from ELF observations. *Radio Science,* **35,** 385-394.

Cummins, K.L., M.J. Murphy, E.A. Bardo, W.L. Hiscox, R.B. Pyle and A.E. Pifer, 1998: A combined TOA/MDF technology upgrade of the U.S. National Lightning Detection Network. *J. Geophys. Res*., **103(D8**), 9035-9044.

Davis, C. et al., 2004: The Bow Echo and MCV Experiment (BAMS): Observations and Opportunities. *Bull. Amer. Meteor. Soc.,* in press.

Franz, R.C., R.J. Nemzek, and J.R. Winckler, 1990: Television image of a large upward electrical discharge above a thunderstorm system. *Science, **249**,* 48-51.

Hu, W., S. Cummer, W.A. Lyons and T. E. Nelson, 2002: Lightning Charge Moment Changes for the Initiation of Sprites," *Geophys. Res. Lett., **29**,* 10.1029/2001GL014593.

Huang, E., E. Williams, R. Boldi, S. Heckman, W. Lyons, M. Taylor, T. Nelson and C. Wong, 1999: Criteria for sprites and elves based on Schumann resonance observations. *J. Geophys. Res.,* **104,** 16943-16964.

Jerauld, J, V.A Rakov, M.A Uman, K.J. Rambo, D.M. Jordan, K.L. Cummins and J.A. Cramer, 2005: An evaluation of the performance characteristics of the U.S. National Lightning Detection Network in Florida using rocket-triggered lightning. *J. Geophys. Res.,* 110, D19106, doi: 10.1029/2005JD005924.

Lang, T, L. J. Miller, M. Weisman, S.A. Rutledge, L.J. Barker, III, V.N. Bringi, V. Chandrasekar, A. Detwiler, N. Doesken, J. Helsdon, C. Knight, P. Krehbiel, W.A. Lyons, D. MacGorman, E. Rasmussen, W. Rison, W.D. Rust and R.J. Thomas, 2004: The Severe Thunderstorm Electrification and Precipitation Study (STEPS), *Bull. Amer. Meteor. Soc.*, (in press).

Lang, T.J., S.A. Rutledge and K.C. Wiens, 2004: Origins of positive cloud-to-ground lightning flashes in the stratiform region of a mesoscale convective system. *Geophys. Res. Lett.,* **31,** L10105, doi:10.1029/2004GL019823,2004.

Lyons, W.A., 2006: The Meteorology of Transient Luminous Events – An Introduction and Overview, Chapter 1, NATO Advanced Study Institute on Sprites, Elves and Intense Lightning Discharges, M. Fullekrug, Ed., Corte, Corsica, 37 pp.

Lyons, W.A. and S.A. Cummer, 2005: Lightning characteristics of the Aurora, NE record hail stone producing supercell of 22-23 June 2003 during BAMEX. 1st Conf. on Meteorological Applications of Lightning Data, AMS, San Diego (available on conference preprint CD).

Lyons, W.A. and R.A. Armstrong, 2004: A review of electrical and turbulence effects of convective storms on the overlying stratosphere and mesosphere. *AMS Symposium on Space Weather,* AMS Annual Meeting, Seattle, 6 pp, CD.

Lyons, W.A., T.E. Nelson, R.A. Armstrong, V.P. Pasko, and M. Stanley, 2003a: Upward electrical discharges from the tops of thunderstorms. *Bull. Amer. Meteor. Soc.,* **84**, 445-454.

Lyons, W.A., T.E. Nelson, E.R. Williams, S. A. Cummer and M.A. Stanley, 2003b: Characteristics of sprite-producing positive cloud-to-ground lightning during the 19 July STEPS mesoscale convective systems. *Mon. Wea. Rev.,* **131***,* 2417-2427.

Lyons, W.A., T.E. Nelson, E.R. Williams, J. A. Cramer and T.R. Turner, 1998: Enhanced Positive Cloud-to-Ground Lightning in Thunderstorms Ingesting Smoke from Fires. *Science* , 77-80.

Lyons, W.A., M. Uliasz and T.E. Nelson, 1998: climatology of large peak current cloud-to-ground lightning flashes in the contiguous United States. *Mon. Wea. Rev. ,* **126**, 2217-2233.

Lyons, W.A., 1996: Sprite observations above the U.S. High Plains in relation to their parent thunderstorm systems, *J. Geophys. Res.* **101,** 29,641-29,652.

Pasko, V.P., U.S. Inan and T.F. Bell, 1996: Sprites as luminous columns of ionization produced by quasi-electrostatic thunderstorm fields. *Geophys. Res. Lett.,* **23**, 649-652.

Pasko, V.P., U.S. Inan and T.F. Bell, 1996: Sprites as luminous columns of ionization produced by quasi-electrostatic thundercloud fields. *Geophys. Res. Lett*., **23**, 649-652.

Rakov, V.A. and M. A. Uman, 2003: *Lightning: Physics and Effects*. Cambridge University Press, 687 pp.

Rodger, C.J., 1999: Red sprites, upward lightning and VLF perturbations. *Reviews of Geophysics,* **37,** 317-336.

Rowland, H.L., 1998: Theories and simulations of elves, sprites and blue jets. *J. Atmos. Solar-Terr. Phys.*, **60,** 831-44.

Schuur, T.J. and S.A. Rutledge, 2000: Electrification of stratiform regions in mesoscale convective systems, Part 1: An observational comparison of symmetric and asymmetric MCSs. *J. Atmos. Sci.,* **57***,* 1961-1982.

Stanley, M.A., 2000: *Sprites and their parent discharges.* Ph.D. Dissertation, New Mexico Institute of Mining Technology, Socorro, NM, 163pp.

Thomas, R.J., P.R. Krehbiel, W. Rison, S.J. Hunyady, W.P. Winn, T. Hamlin and J. Harlin, 2004: Accuracy of the Lightning Mapping Array. *J. Geophys. Res.,* **109,** D14207, doi: 10.1029/2004JD004549,2004.

Williams, E.R., 1998: The positive charge reservoir for sprite-producing lightning. *J. Atmos. Sol. Terr. Phys.,* **60***,* 689-692.

Wilson, C.T.R., 1925: The electric field of a thunderstorm and some of its effects. *Proc. Phys. Soc. Lond.,* **37***,* 32D-37D.

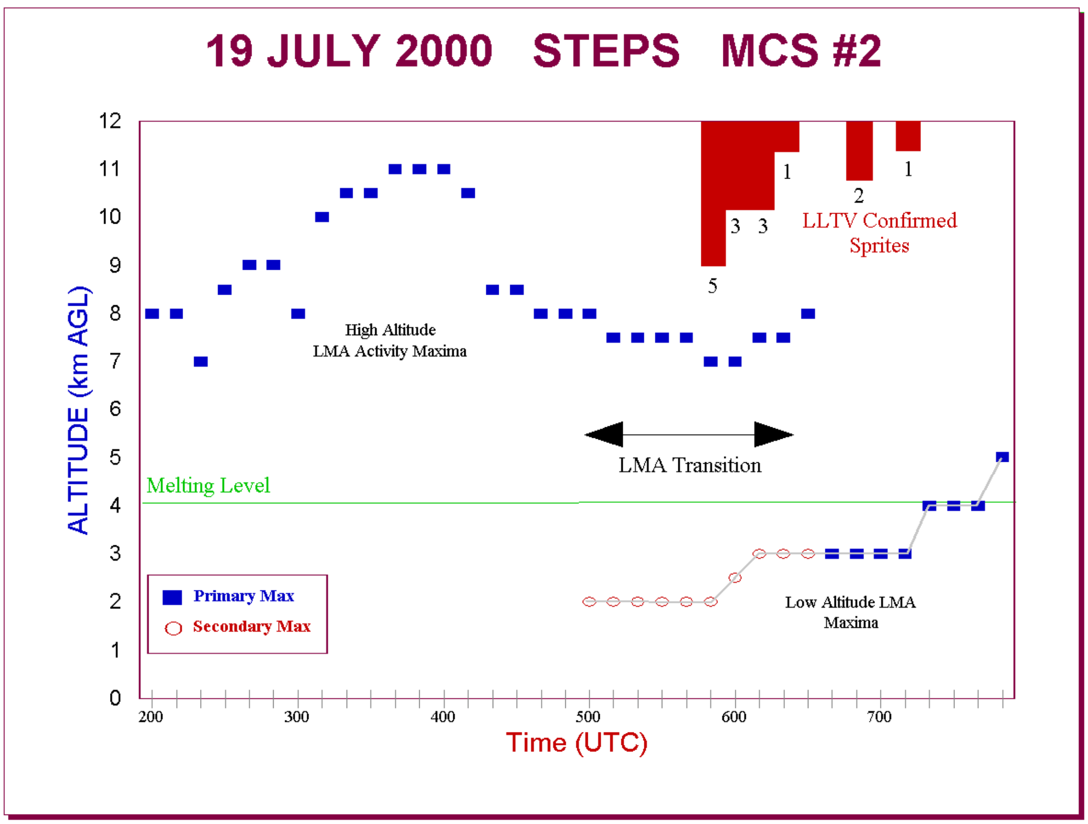

Figure 1. Centroid of VHF source maxima as a function of time for the MCS of 19 July 2000 in the STEPS domain. Numerous positive CGs created no sprites until a region of low-level electrical activity started to assume dominance after 0500Z (from Lyons et al. 2003b).

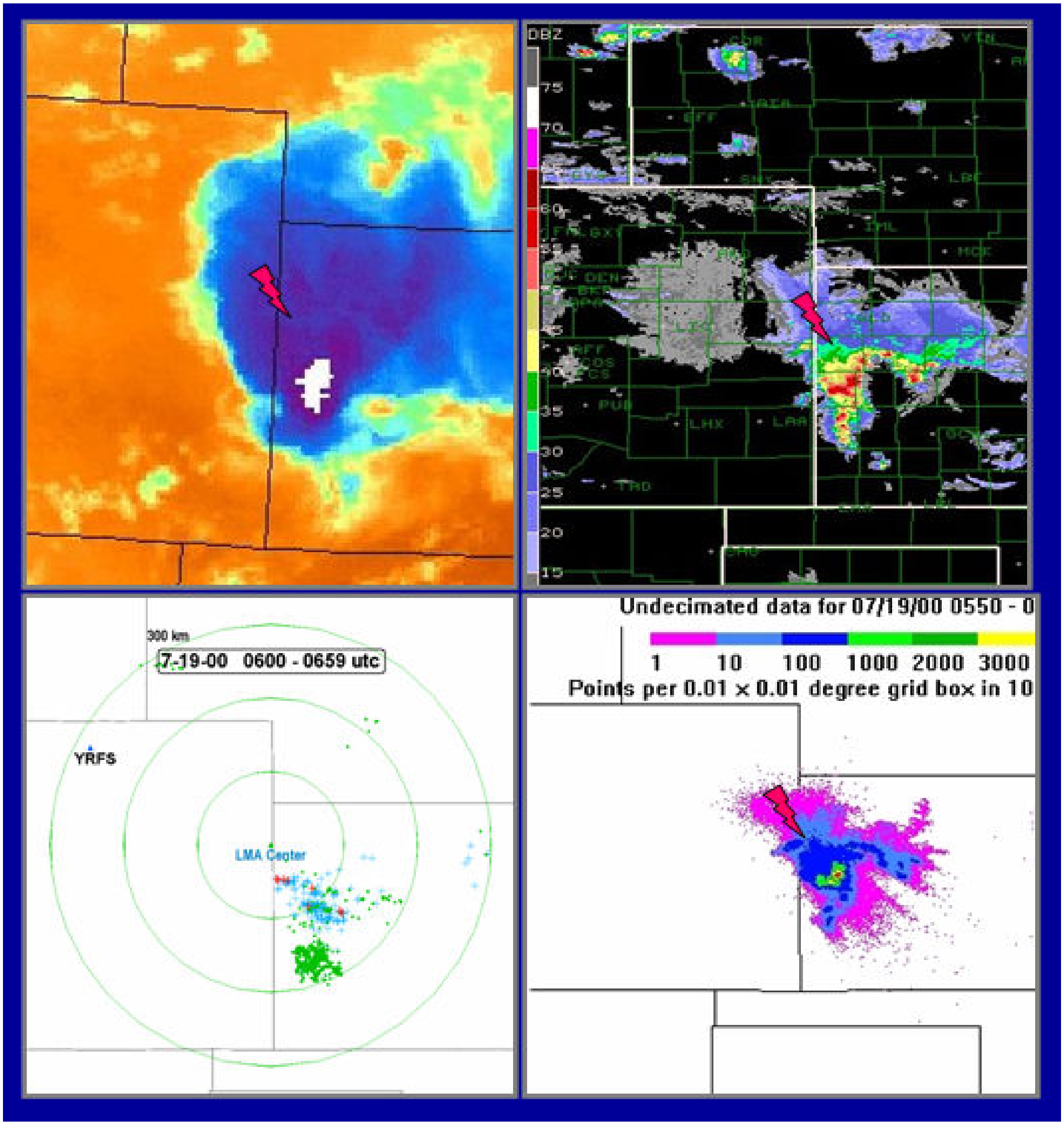

Figure 2 (upper left). Location of a 30 kA sprite parent +CG at 0600.15.346 UTC 19 July 2004 (red lightning symbol), occurring several tens of kilometers north of the coldest cloud tops (white). Figure 3 (upper right). NEXRAD reflectivity mosaic at 0600 UTC showing sprite +CG occurred in the low reflectivity stratiform region of the MCS. Figure 4 (lower left) Plot of CGs from 0600 to 0700, with –CGs (green) in storm's core, +CGs (blue) mostly in the stratiform region and sprite parent +CGs (red). Figure 5 (lower right). Density plot of LMA VHF sources from 0550-0600 UTC showing the sprite event occurred well north of the region of maximum storm electrical activity.

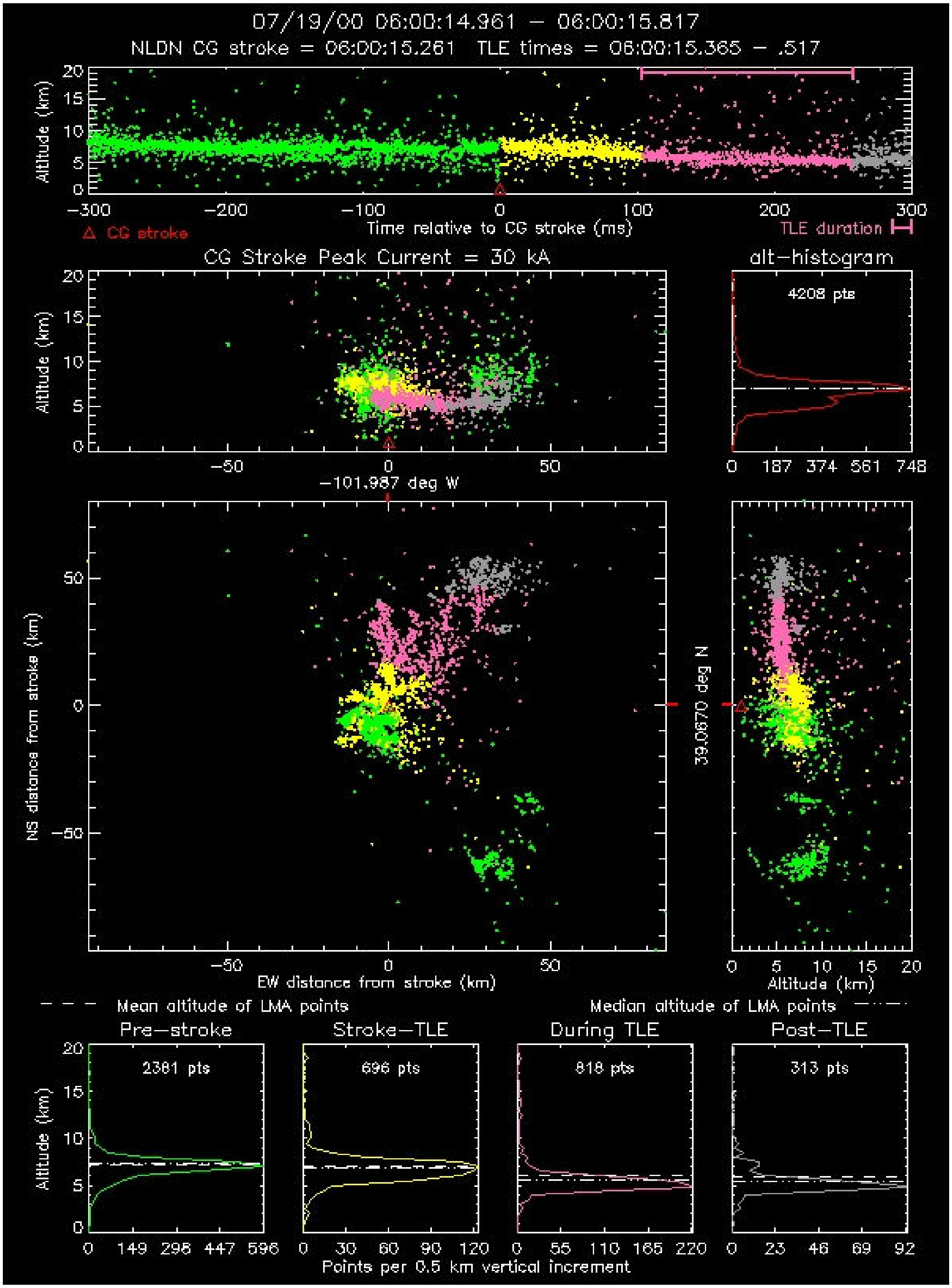

Figure 6. LMA display of the entire discharge associated with the 0600.15 UTC sprite on 19 July 2000. The green VHF sources are for the initial period before the +CG return stroke. The yellow dots are sources during the period from the +CG return stroke to the onset of sprite luminosity. The pink dots are the VHF sources during the period the sprite was detected optically, and the grey dots are those source after the sprite had dimmed.

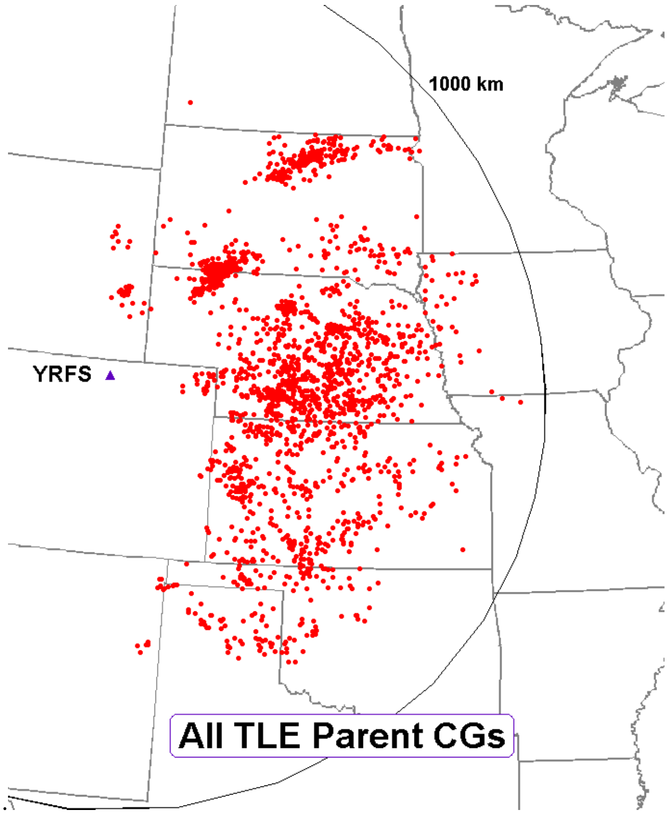

Figure 7. Plot of parent +CG locations of 2219 TLEs (mostly pure sprites) observed using low light cameras from the Yucca Ridge Field Station near Fort Collins, 1995-2004, but primarily from the STEPS 2000 campaign.

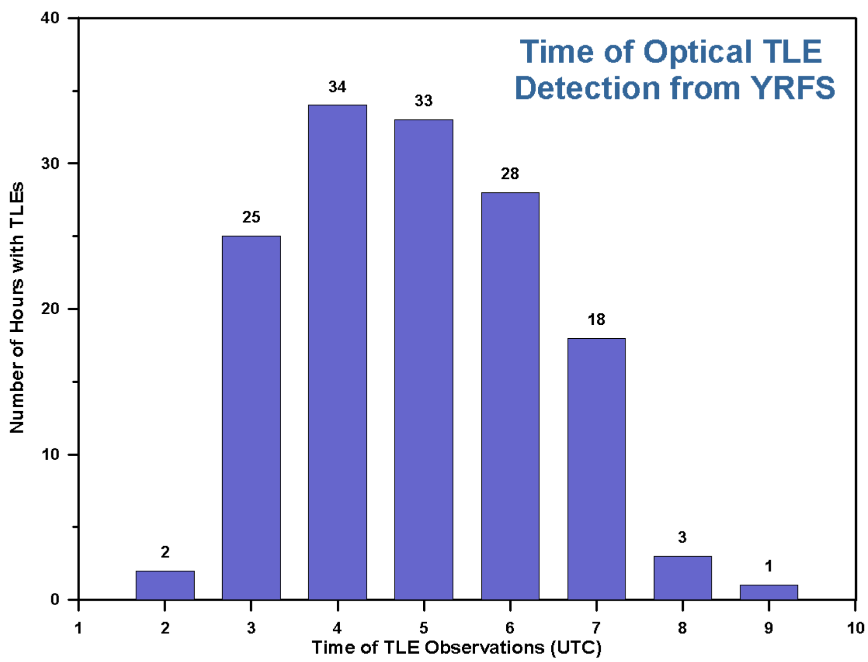

Figure 8. The hours (UTC) during which TLEs were observed using LLTV systems at the Yucca Ridge Field Station. Summer sunset is usually between 0230-0330 UTC, with sunrise starting around 1000 UTC.

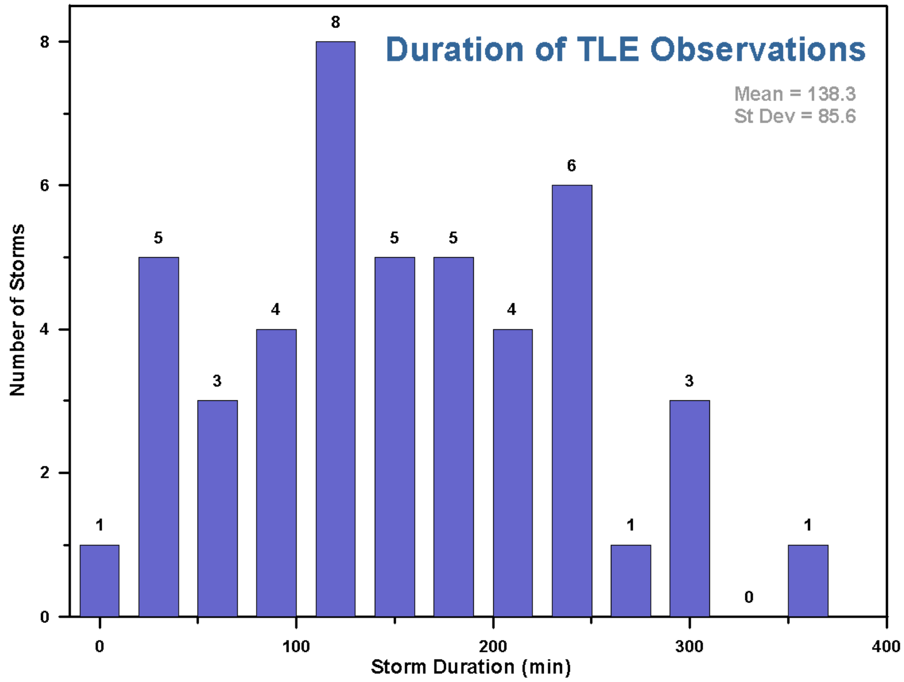

Figure 9. The durations (in 30 minute segments) of TLE production optically confirmed for storms over the U.S. High Plains.

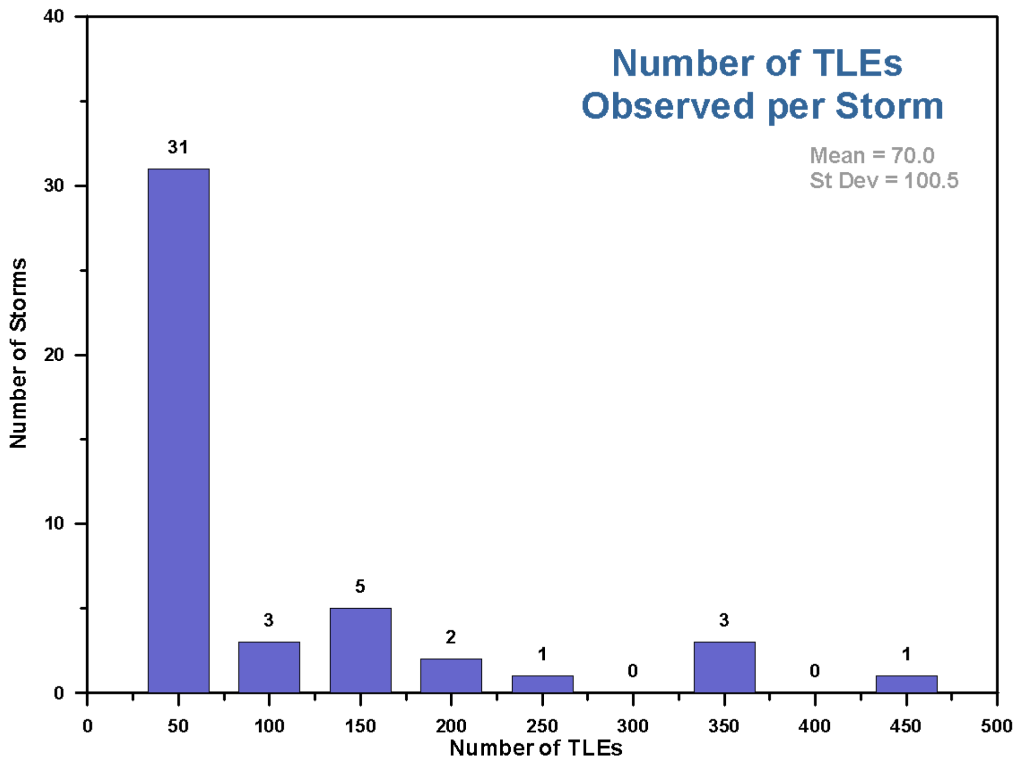

Figure 10. Histogram of the number of TLEs per active storm (increments of 50) for summer convective systems over the U.S. High Plains.

||

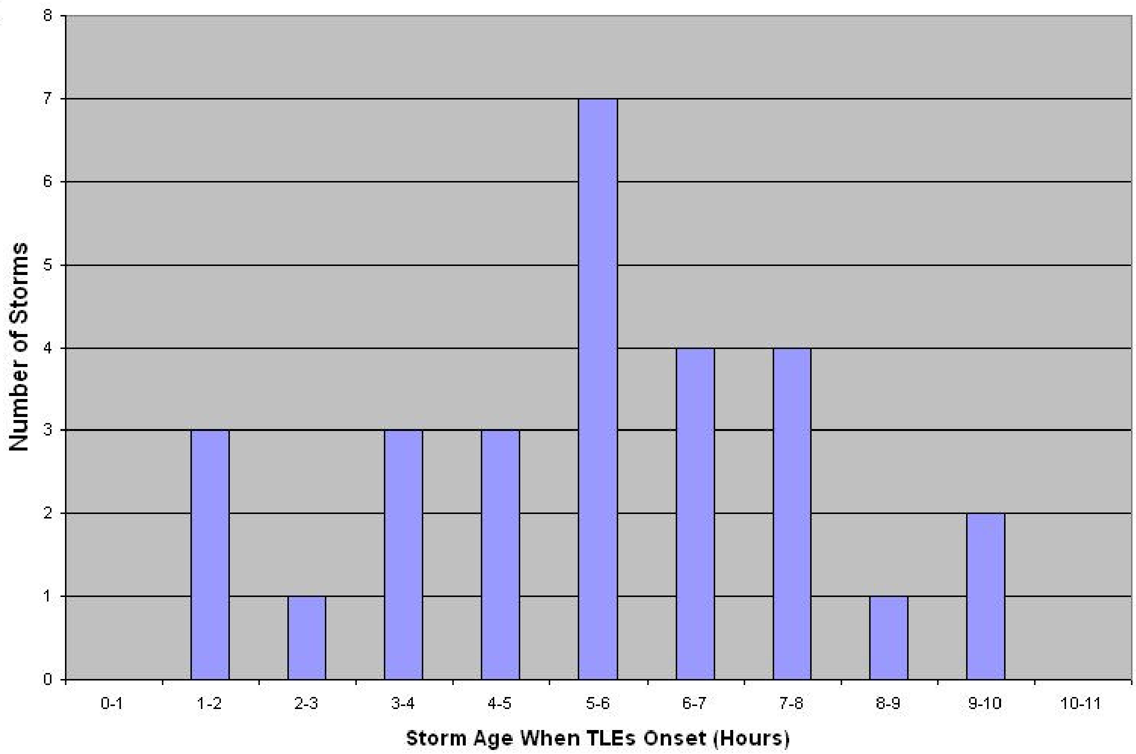

Figure 11. The age of the parent storm at the time of detection of the first TLE during summer storms over the U.S> High plains.

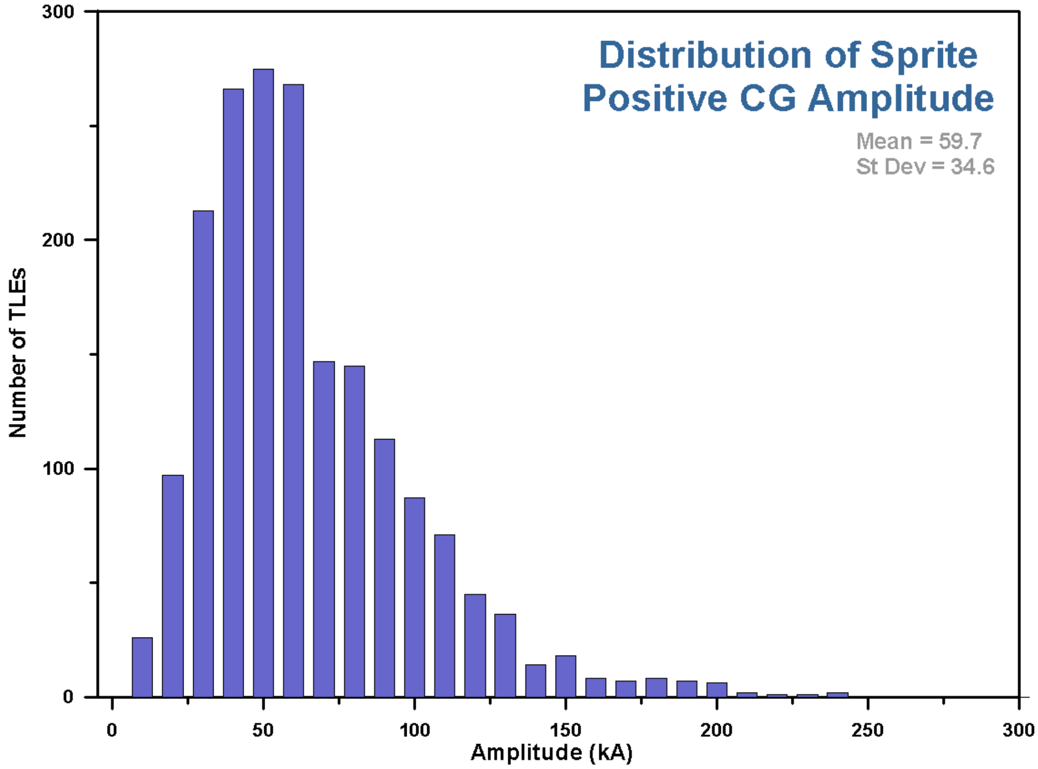

Figure 12a. Distribution (10 kA increments) of NLDN +CG peak currents for sprites events.

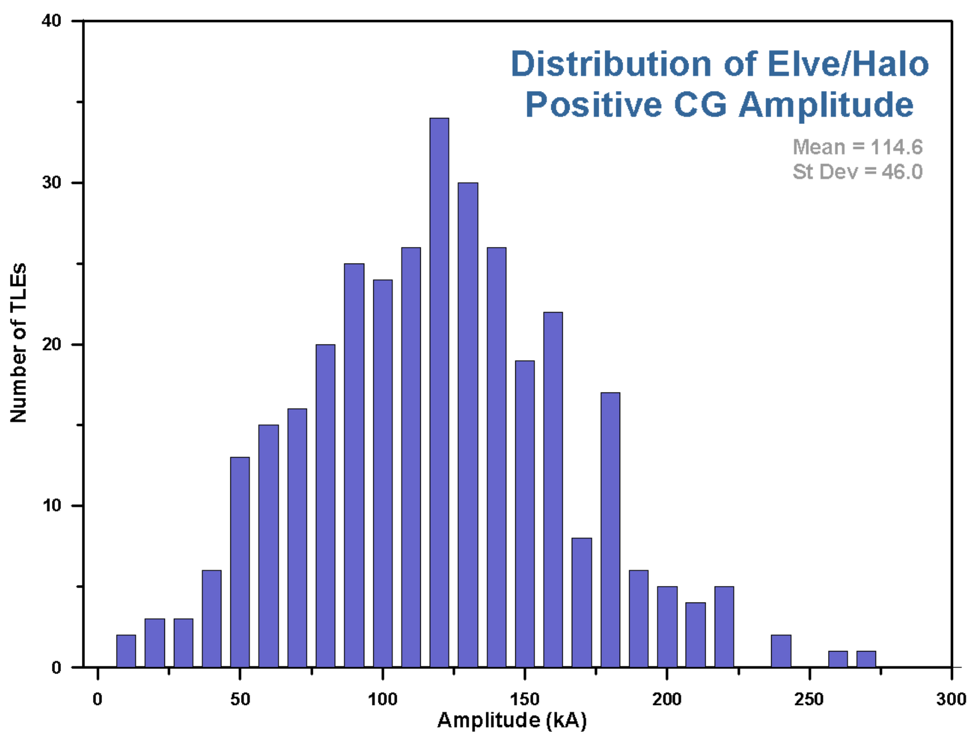

Figure 12b. Distribution (10 kA increments) of NLDN +CG peak currents for TLEs containing elves and halos, some of which were followed by sprites.

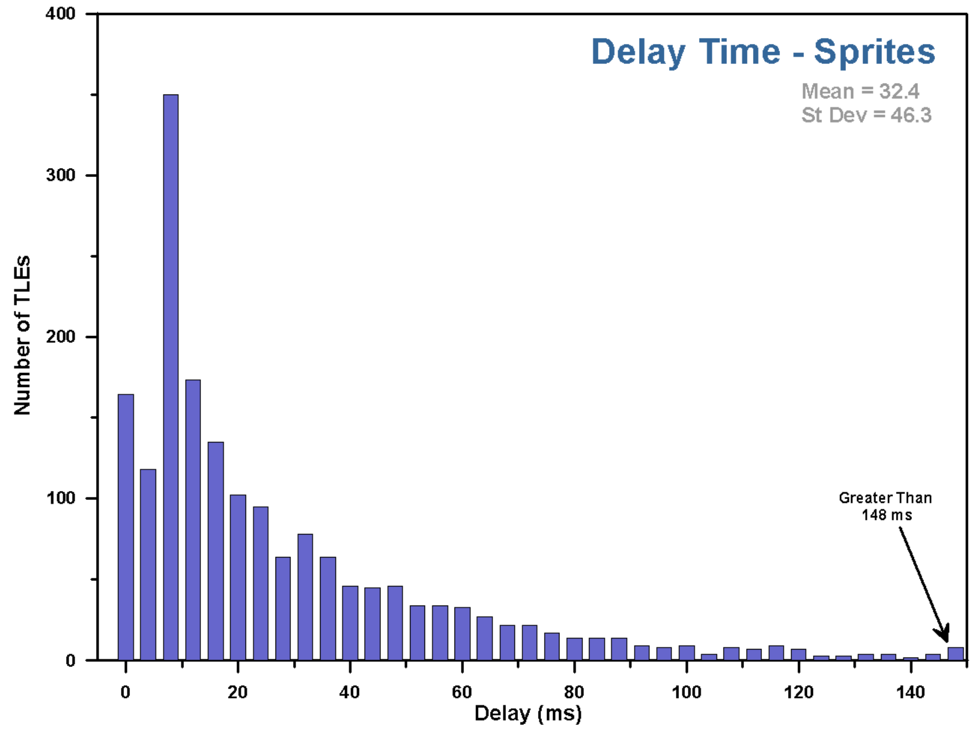

Figure 13. The estimate delay time (ms) between the sprite parent +CG and the onset of sprite luminosity.

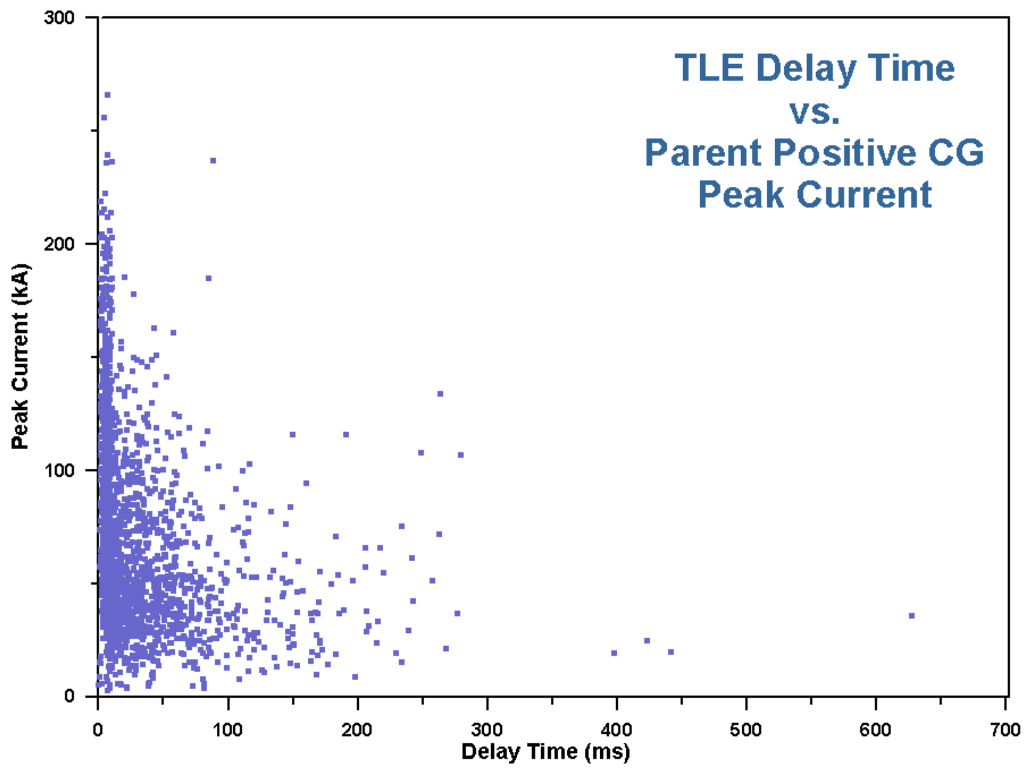

Figure 14. The TLE parent +CG peak currents plotted versus the estimated delay time (ms).

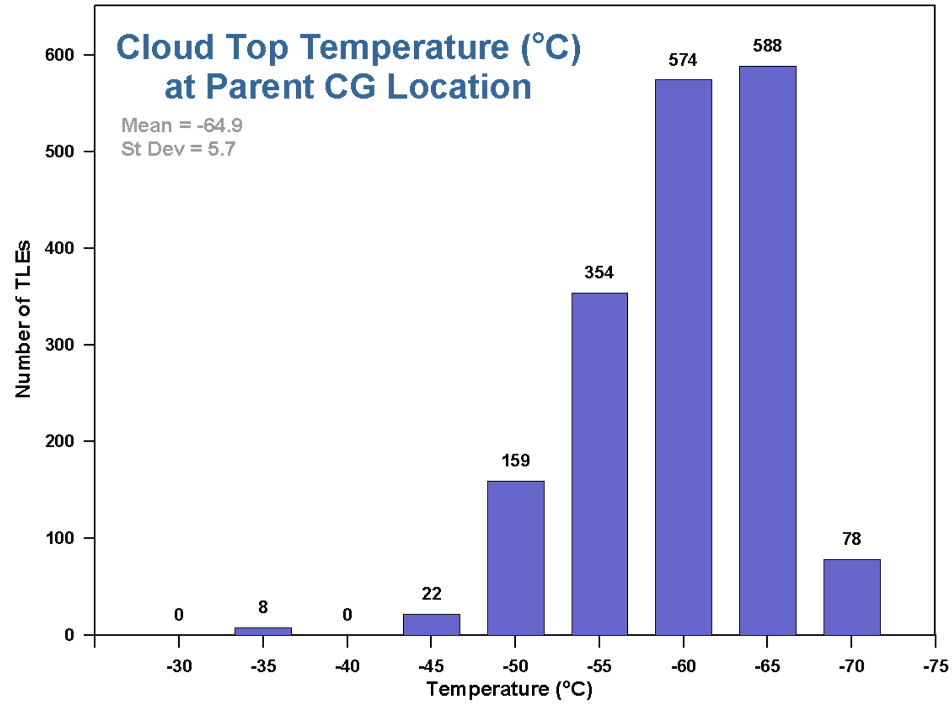

Figure 15. Distribution of cloud top canopy infrared temperatures above the location of TLE parent +CGs.

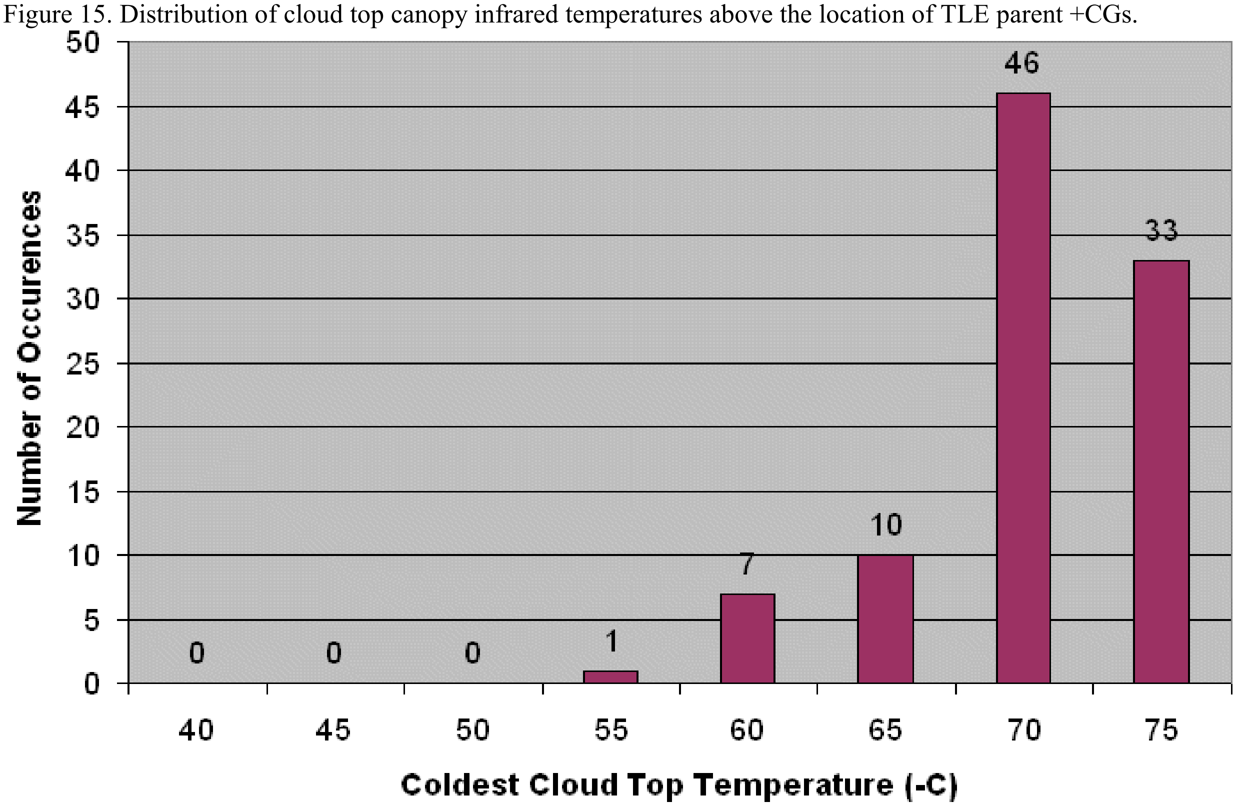

Figure 16. Distribution of coldest IR cloud top temperature anywhere in a convective system producing TLEs at the time over the U.S. High plains during summer.

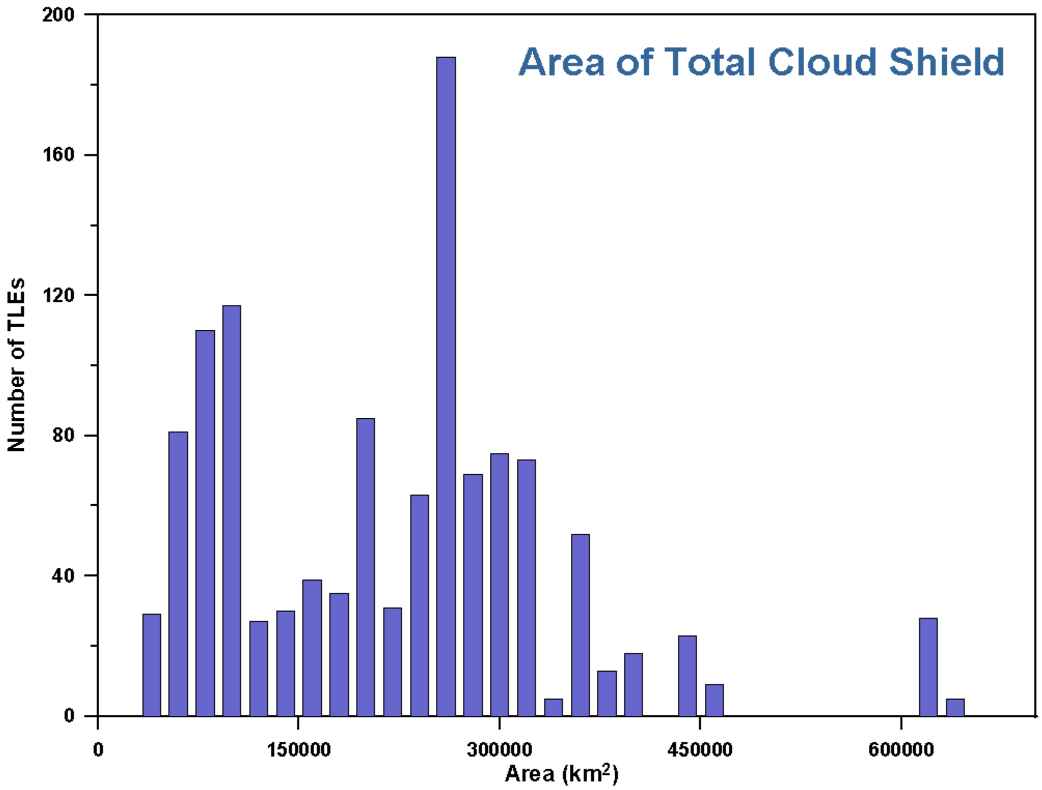

Figure 17. Area of the GOES IR cloud shield (roughly the -30°C contour) versus the number of TLEs. All storm systems were >20,000 km^2.

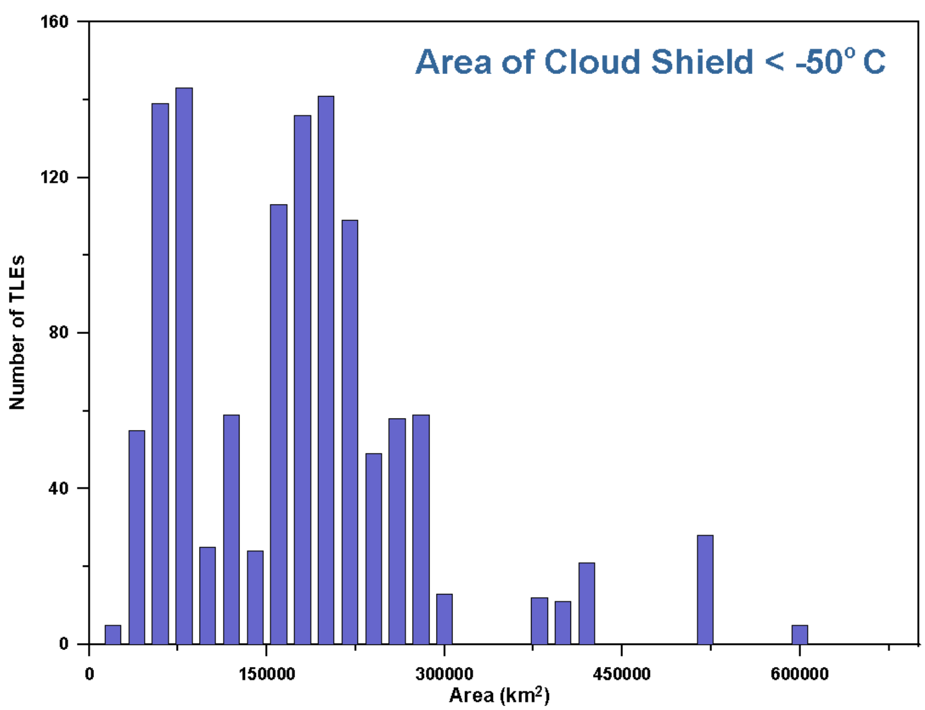

Figure 18. Area of the GOES IR cloud shield colder than -50°C versus the number of TLEs. Very few TLEs occurred from storms having warmer cloud tops.

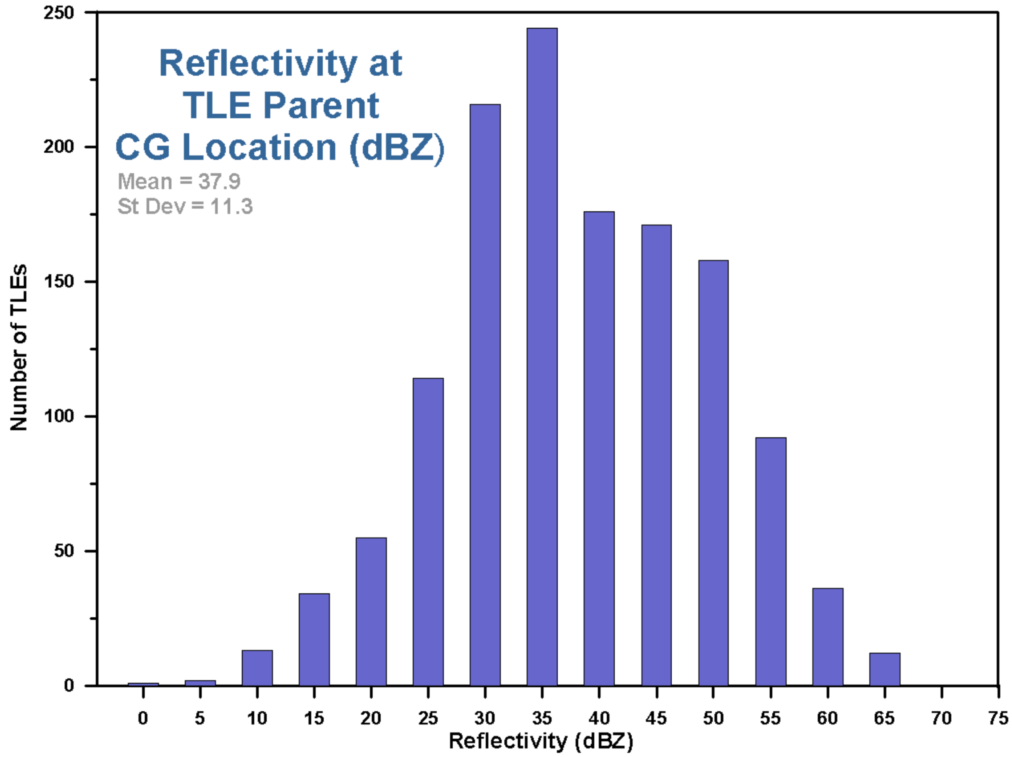

Figure 19. Distribution of the NEXRAD base reflectivities (dBZ) at the locations of the TLE +CG.

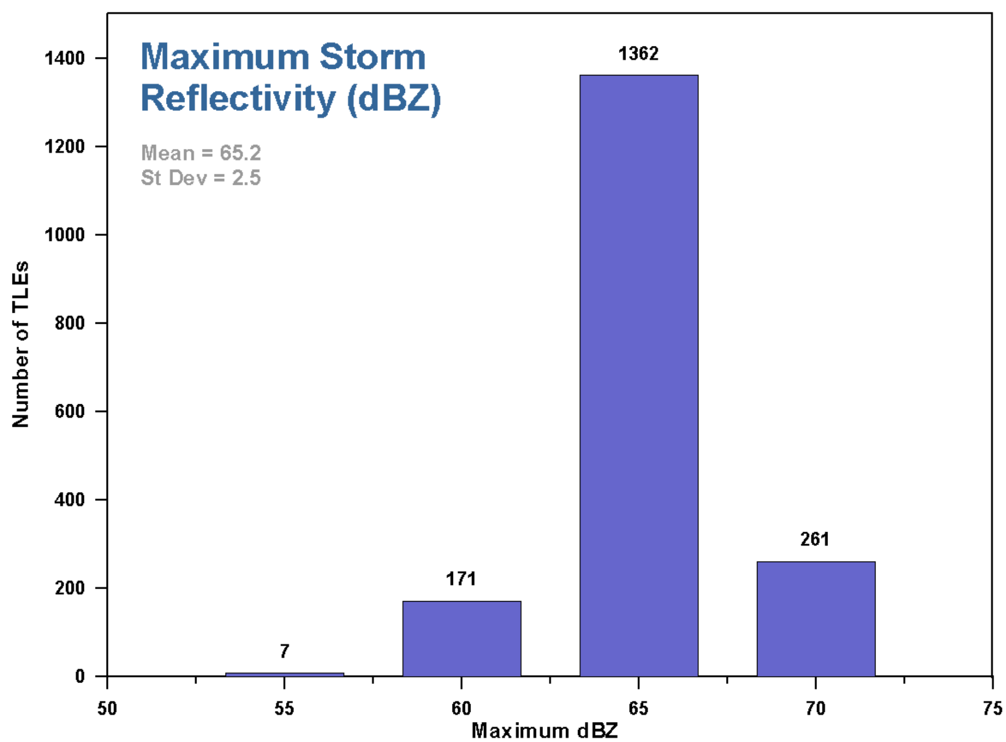

Figure 20. Distribution of the highest NEXRAD base reflectivity anywhere in the convective system while TLEs were being observed optically.

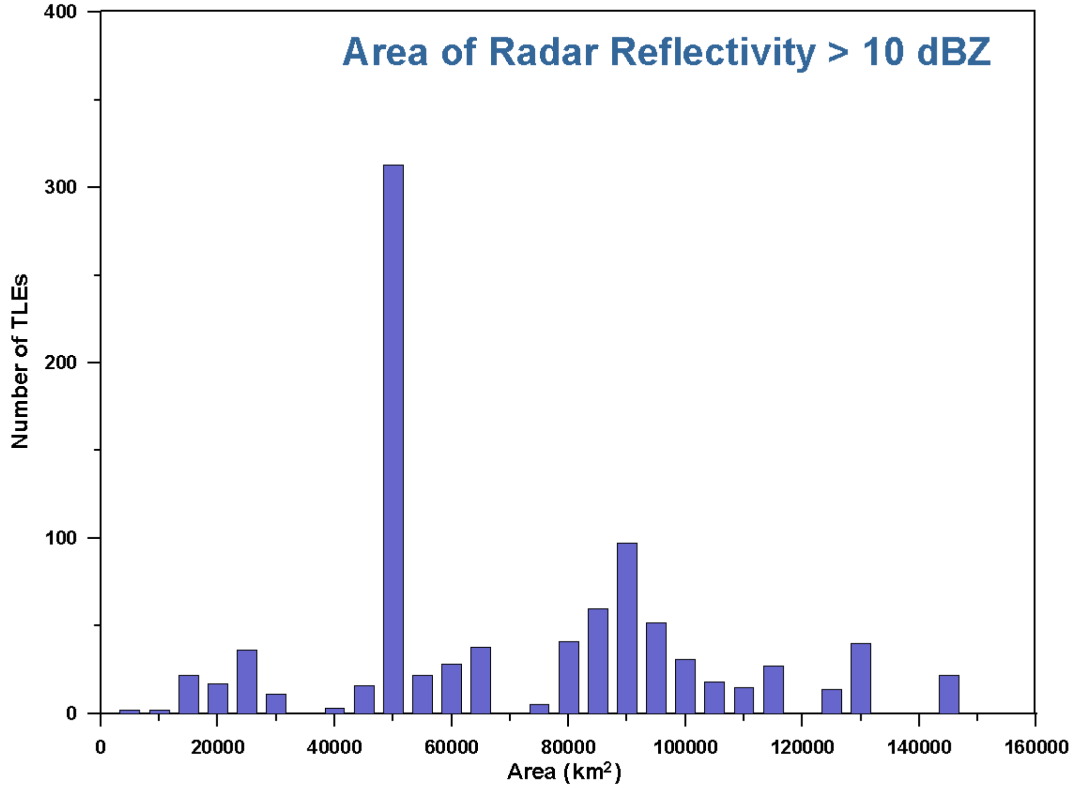

Figure 21. Area of the radar echo > 10 dBZ versus the number of observed TLEs. Few events were noted for systems smaller than 20,000 km^2.

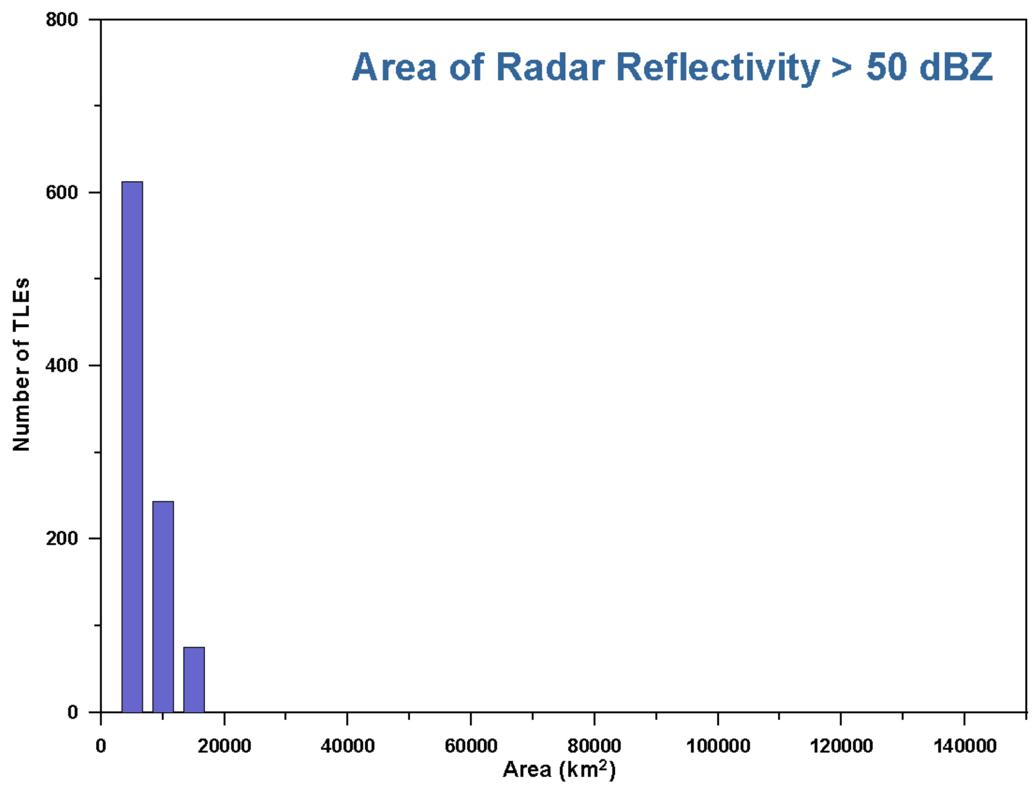

Figure 22. The echo area >50 dBZ in storms from which TLEs were being observed.

Relative Brightness vs. dBZ

5	4	10	12	33	73	60	40	23	17	7	1	2	0	0
4	3	10	18	27	59	68	52	31	21	14	4	3	0	0
3	3	8	21	35	56	71	47	40	31	17	9	2	0	0
2	3	7	20	29	50	53	51	50	44	27	9	4	0	0
1	2	3	17	23	33	41	45	40	44	26	13	1	0	0
	10	15	20	25	30	35	40	45	50	55	60	65	70	75

All TLEs

Normalized values of relative brightness vs. dBZ

5	0.3%	0.6%	0.8%	2.1%	4.7%	3.8%	2.5%	1.5%	1.1%	0.4%	0.1%	0.1%	0.0%	0.0%
4	0.2%	0.6%	1.1%	1.7%	3.8%	4.3%	3.3%	2.0%	1.3%	0.9%	0.3%	0.2%	0.0%	0.0%
3	0.2%	0.5%	1.3%	2.2%	3.6%	4.5%	3.0%	2.5%	2.0%	1.1%	0.6%	0.1%	0.0%	0.0%
2	0.2%	0.4%	1.3%	1.8%	3.2%	3.4%	3.2%	3.2%	2.8%	1.7%	0.6%	0.3%	0.0%	0.0%
1	0.1%	0.2%	1.1%	1.5%	2.1%	2.6%	2.9%	2.5%	2.8%	1.7%	0.8%	0.1%	0.0%	0.0%
	10	15	20	25	30	35	40	45	50	55	60	65	70	75

Figure 23. Matrix of the relative brightness (1 to 5 scale) of TLEs versus the NEXRAD base reflectivity (dBZ) at the location of the TLE parent +CG. The brightest events are most prevalent at relative low reflectivity values.

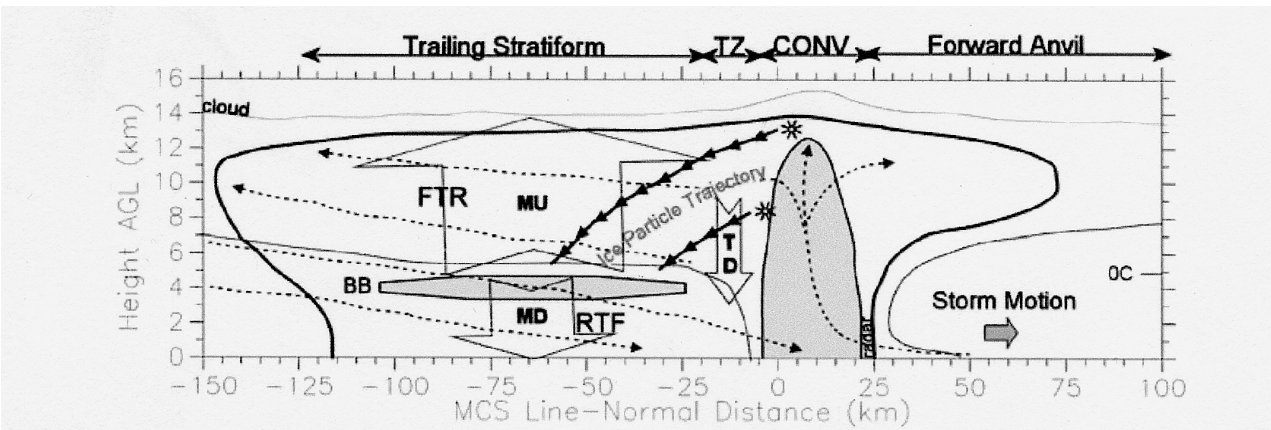

Figure 24. Idealized structure of an MCS with a leading convective core and a trailing stratiform region (from Carey et al. 2005). In their case study of the 16 June 2002 MCS above an LDAR II in north Texas, large discharges were mapped originating near the top of the convective core and descending rearward into the bright band layer where a +CG event occurred. We believe many prototypical spites discharges may occur in this manner.